Behavior and alpha-band oscillations reveal cross-modal interactions between chemosensory and auditory processing

Laura-Isabelle Klatt*,† & Christine Hucke**,†

Leibniz Research Centre for Working Environment and Human Factors

* Correspondence: klatt@ifado.de
** Correspondence: hucke@ifado.de
† Both authors contribute equally

Summary

The perceived location of a sound can be mislocated towards a spatially discordant but temporally synchronous visual stimulus. This is referred to as the spatial ventriloquist effect. However, whether chemosensory cues can similarly bias sound localization remains largely unaddressed. Hence, the present EEG study adopted a dynamic sound localization paradigm with concurrent bimodal odorant stimulation. Participants heard sequences of sounds varying in location. After each sound, participants made a two-alternative forced choice localization judgment (left vs. right). Critically, in a subset of occasions, but unbeknown to the participants, the sounds originated from a central location. Furthermore, in the first half of the sequence, sound presentation could be accompanied by a task-irrelevant, trigeminally potent odorant in the left, right, or both nostril(s). Auditory-only trials and birhinal stimulation served as controls. For central sounds in the second half of the sequence, the proportion of right-ward responses increased with right-nostril stimulation but decreased with left-nostril stimulation relative to the control conditions, showing an after-effect of odorant stimulation for ambiguous sound cues. This odorant-induced localization bias diminished with increasing spatial discernability of the sounds. On the contrary, alpha power lateralization, a correlate of auditory spatial attention, was most susceptible to odorant stimulation when the spatial disparity between the senses was largest, as reflected in diminished alpha lateralization for incongruent chemosensory-sound stimulation. No such effect was present in a multivariate decoding analysis of alpha power. We discuss the present findings in light of cross-modal interactions and a proposed common attentional control system between the senses.

Keywords: spatial ventriloquism effect, cross-modal interactions, spatial attention, chemosensory, sound localization, alpha lateralization, multivariate pattern analysis

1. Introduction

When conflicting sensory information is processed through different senses, we may observe that one sensory domain influences or biases the other domain. For instance, in the audiovisual domain, the 'spatial ventriloquism effect' describes how the perceived location of a sound is shifted towards a concurrently presented but spatially divergent visual stimulus (for a review, see[1]). The ventriloquism effect has also been investigated in other modalities, such as the visuo-tactile domain[2], but to a lesser extent. In contrast, much less is known about the interaction between our chemical senses and other sensory modalities.

To date, a limited number of studies has revealed cross-modal interactions between olfaction and vision, showing that odorant stimulation can modulate visual motion processing[3] as well as visuo-spatial navigation[4]. Focusing on cross-modal interactions between chemosensation and audition, a behavioral study by Liang and colleagues[5] recently investigated whether odorants can bias the perceived location of a centrally presented sound towards the stimulated nostril. Specifically, the participants' left or right nostril was stimulated with a pure olfactory stimulus (phenylethyl alcohol, rose smell) or a bimodal (i.e., olfactory-trigeminal) stimulus (menthol, mint smell) while performing a two-alternative forced choice sound localization task (left versus right). The authors found that centrally presented sounds were more frequently categorized as originating from the right side if participants received monorhinal rightward odorant stimulation. Critically, the odorant-induced sound localization bias was only present with a bimodal olfactory-trigeminal stimulus but not with a pure olfactory stimulus. In line with research showing that humans can only localize monorhinally presented odors when they stimulate the trigeminal system[6–8], this demonstrates that trigeminal stimulation is essential to evoke a chemosensory spatial ventriloquism effect.

While the findings by Liang and colleagues[5] clearly demonstrate the influence of trigeminal cues on the perception of ambiguous sound sources, the underlying electrophysiological mechanisms have not been investigated to date. Hence, the aim of the current study is two-fold: First, we aim to replicate the behavioral odorant-induced sound localization bias found by Liang et al., using a different bimodal stimulus (i.e., isopropanol) and a modified, EEG-compatible design. Further, we aim to shed light on the underlying neurocognitive mechanisms, focusing on the modulation of univariate and multivariate EEG-correlates of spatial attention. Specifically, the present investigation focuses on attentional modulations of alpha oscillations.

An abundant body of research has linked hemispheric modulations of alpha power to the allocation of spatial attention in various domains, such as anticipatory shifts of spatial attention[9–12], attentional orienting within working memory[13–16], or attentional selection from a stimulus array[17,18]. Across those domains, converging evidence has shown similar patterns of parieto-occipital alpha power lateralization for visual[10,14,15] and auditory[19–22] shifts of covert spatial attention. Together with other neuroimaging findings, this has amounted to the notion of a common supramodal attention system[23, but see also 24,25]. In the last years, increasing popularity of machine learning classification methods have further resulted in a surge of studies showing that the locus of spatial attention can be decoded from the pattern of alpha activity across the scalp[26–30].

Adopting a cross-modal perspective, investigations of alpha power modulations are mainly situated in the context of intersensory orienting (i.e., concerning shifts of attention from one

modality to another), proposing its involvement in the inhibition of processing in task-irrelevant sensory cortices and the re-allocation of resources across sensory systems[31–34]. However, to date, it remains unknown whether alpha power lateralization or classification accuracy based on multivariate alpha power signals are susceptible to cross-modal interactions between a task-relevant and a task-irrelevant modality during the deployment of spatial attention, as reflected in the spatial ventriloquism effect.

Therefore, in the present study, participants completed a sound localization paradigm, in which they were presented with a sequence of sounds from various lateralized locations (see Figure 1-B). After each sound presentation, participants made a two-alternative forced choice judgement, indicating the spatial location of the sound as coming from the left or right side. Critically, in a subset of occasions, but unbeknown to the participants, the sounds were presented at a central location, creating a situation of maximal spatial uncertainty. Sounds were grouped into a sequence of eight consecutive tones (Figure 1-C). Concurrently, during the first half of the sequence, sound presentation could be accompanied by bimodal odorant stimulation in the left, right, or both nostrils (Figure 1-D). In addition to the birhinal stimulation condition, a subset of auditory-only trials served as a neutral control condition. Participants were informed that the chemosensory stimulation was task-irrelevant.

In line with the results by Liang and colleagues[5], we expect that monorhinal stimulation biases the reported sound localization towards the stimulated nostril, especially under conditions of high spatial uncertainty. More precisely, for centrally presented sounds, we expect an increase of right-ward judgements during right-nostril stimulation and a decrease of right-ward indications during left-nostril stimulation. Analogously, faster responses are expected when participants classify a centrally presented sound in accordance with the side of odorant stimulation (congruent trials) as opposed to incongruent responses or responses in the control conditions. The impact of odorant stimulation on sound localization is expected to substantial decrease or potentially disappear at farther lateralized sound locations with little to now spatial uncertainty. We further contrast responses for sounds that were directly paired with an odorant stimulation and those who might be affected by the after-effect of the stimulation that usually out-lasts the actual stimulation[35,36].

On the electrophysiological level, we aim to show whether alpha power lateralization during shifts of auditory spatial attention is boosted by a congruent, lateral odorant stimulation or diminished by an incongruent odorant in comparison to a spatially unspecific odorant condition and a control condition without any odorant stimulation. In addition, to fully exploit the multivariate nature of the EEG recordings, we apply a pattern classification routine to decode the locus of auditory spatial attention from the scalp topography of alpha-band power, while participants receive congruent or incongruent odorant stimulation. Previously, it has been shown that such multivariate measures can be sensitive to effects that are not reflected in univariate measures of spatial attention[29].

To foreshadow the main findings, the present results substantiate previous behavioral evidence for an odorant-induced sound localization bias when spatial cues in the auditory domain are extremely ambiguous. Critically, we show that the magnitude of alpha power lateralization is modulated by the spatial congruency of sound-odor-stimulation at outer (+/-15° azimuth), but not at inner (+/-5° azimuth) or central (0° azimuth) sound locations. Multivariate decoding of auditory spatial attention was diminished by concurrent odor-

stimulation; however, this remained insensitive to the differences between the odor-stimulation conditions. Taken together, the present study provides compelling evidence for a spatial ventriloquism effect in the auditory-chemosensory domain and for the first time, sheds light on the underlying electrophysiological underpinnings. The findings present an important contribution to our understanding of cross-modal interactions between auditory perception and chemosensory processing.

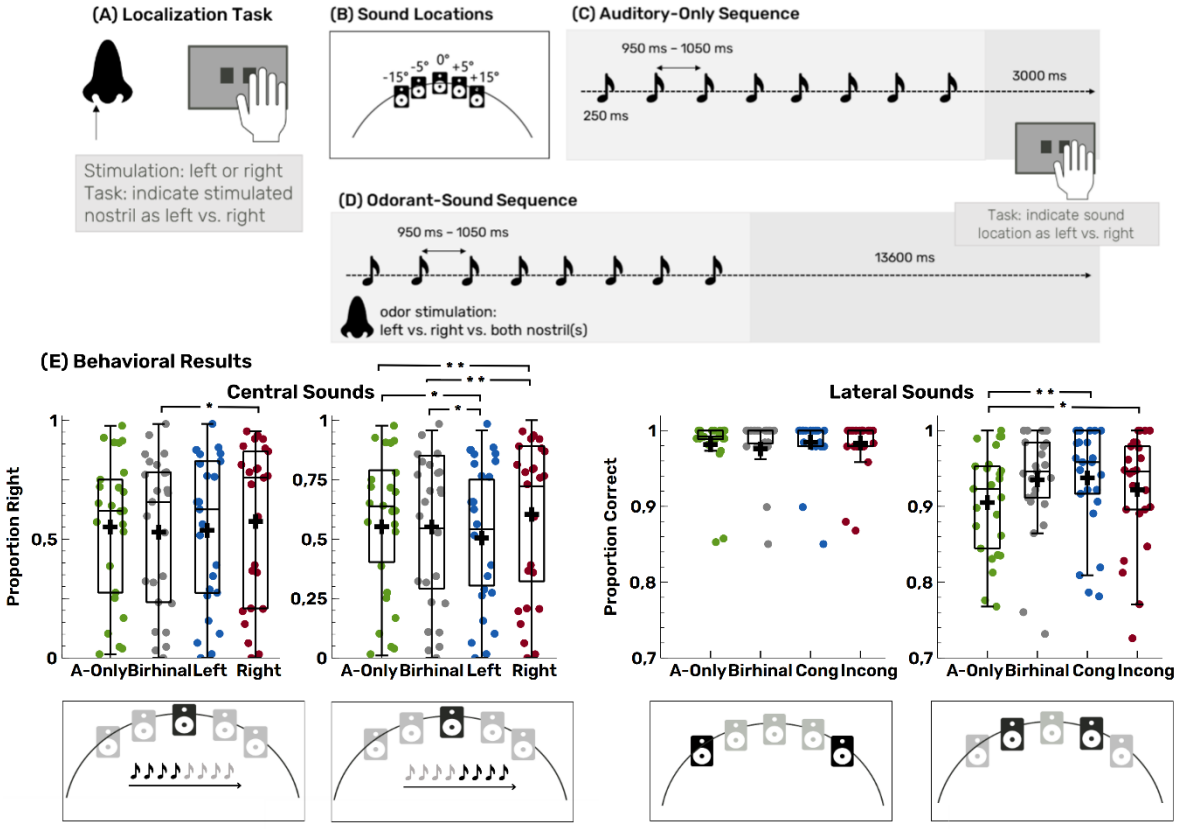

Figure 1. Localization judgements in dynamic sound localization paradigm is modulated by an after-effect of monorhinal bimodal odorant stimulation when sound cues are highly ambiguous. (A) To determine the concentration that is trigeminally potent for each individual subject, participants completed an odorant localization task in the beginning of the experiment. (B) During the sound localization paradigm, sounds could be presented at five different location (-15°, -5°, 0°, +5°, -15° azimuth in the horizontal plane). (C) Schematic illustration of an auditory only sound sequence of eight tones. Participants were required to indicate the perceived direction of the sound (left vs. right) via button press with their dominant hand of. The inter stimulus interval was between 950 and 1050 ms and the inter sequence interval was 3 s. (D) Illustration of a sound sequence that was accompanied by a bimodal odorant stimulation either in the left, right, or both nostril(s). The inter-sequence interval was 13.6 s. (E) Boxplots illustrate the proportion of right-button presses for centrally presented sounds (left) and the proportion of correct responses for the lateralized sounds (right). Lines in the boxplots indicate the median whereas the plus indicates the mean, and whiskers denote +-1.5 IQR. * p < .05, ** p <.01 in one-sided post hoc planned contrasts. Cong = Congruent, Incong = Incongruent, A-only = Auditory-only.

2 Results

2.1 Behavioral Results

After-effect of monorhinal trigeminal stimulation biases sound localization when sound cues are highly ambiguous

A two-way rmANOVA (stimulation x sequence half) on the proportion of right-ward judgements in response to central sounds was conducted to assess the influence of odorant-stimulation on sound localization under conditions of high spatial uncertainty. While there was no significant main effect of *sequence halves*, $F(1,72) = 0.112$, $p = .741$, $\eta_p^2 = 0.005$, we observed a significant main effect of *stimulation*, $F(3,72) = 4.590$, $p = .005$. $\eta_p^2 = 0.161$, as well as a significant interaction, $F(3,72) = 3.563$, $p = .018$, $\eta_p^2 = 0.129$.

Using planned contrasts, we tested left and right-nostril stimulation against the control conditions (auditory-only, birhinal stimulation), separately for trials within the first and the second half of the sound sequence. In the first sequence half, congruent right-nostril stimulation had an increasing effect on right-ward judgements compared to the birhinal control condition, $t(111.475) = 2.074$, $p = .020$, $d = 0.517$. The other comparisons in the first sequence half were not significant (all $p \geq 0.282$). In line with an after-effect of odorant stimulation, in the second sequence half, left nostril stimulation significantly decreased the proportion of right-ward judgements compared to the birhinal, $t(111.475) = -2.153$, $p = .017$, d = -0.430, and auditory-only control conditions, $t(111.475) = -2.199$, $p = .015$, d = -0.411. In contrast, right-nostril stimulation significantly increased the right-ward indications compared to birhinal stimulation, $t(111.475) = 2.441$, $p = .008$, d = 0.676, and compared to the auditory-only control condition, $t(111.475) = 2.395$, $p = .009$, d = 0.378.

Response times for central sounds are not affected by odorant stimulation

An analogous two-way rmANOVA for reaction times in response to the centrally presented sounds did neither render a significant main effect of *stimulation*, $F(3,60) = 0.861$, $p = .466$, $\eta_p^2 = 0.41$, or of *sequence half*, $F(1,20) = 0.981$, $p = .334$, $\eta_p^2 = 0.047$, nor a significant interaction effect, $F(3,60) = 0.399$, $p = .754$ $\eta_p^2 = 0.020$. This suggests that response times are not affected by odorant stimulation.

Odorant-induced sound localization bias diminishes with increasing spatial discernability of sound cues

To assess whether the observed odorant-induced sound localization bias persists when sound cues become increasingly discernable, we performed a three-way rmANOVA (*stimulation* x *sound position* x *sequence half*) on the proportion of correction responses for lateralized sounds. A significant main effect of *sound position*, $F(1,24) = 34.749$, $p < .001$, $\eta_p^2 = 0.591$, confirms the descriptive pattern of better performance for strongly lateralized (i.e., +/-15°, $M = 98.14\%$, $SD = 4.32\%$) as opposed to less strongly lateralized sounds (i.e., +/- 5°, $M = 92.48\%$, $SD = 6.54\%$, see Figure 1-E). Further, a significant main effect of *stimulation*, $F(2.005,48.130) = 3.243$, $p = 0.048$, $\eta_p^2 = 0.119$, was obtained after Greenhouse-Geisser correction (approx. $\chi^2(5) = 16.613$, $p = .005$, $GG\varepsilon = 0.668$). The latter was modulated by *sound position*, as indicated by

a significant interaction between *stimulation* and *sound position*, $F(3,72) = 5.252$, $p = .002$, $\eta_p^2 = 0.180$. None of the effects involving the factor *sequence half* was significant (all $p \geq .243$).

To resolve the significant interaction between *stimulation* and *sound position*, planned contrasts were applied to test the effect of *stimulation* on the localization of the mid-out and far-out speaker positions, separately. There were no significant differences between the stimulation conditions at far-out speaker positions (all $p \geq 0.255$). However, stimulation influenced localization at mid-out positions significantly. Specifically, compared to an auditory-only control condition, localization accuracy was significantly higher when chemosensory stimulation and sound position were congruent, $t(140.015) = 4.266$, $p < .001$, d = 0.791. Surprisingly, incongruent stimulation also significantly increased localization accuracy compared to an auditory-only control condition, $t(140.015) = -2.221$, $p = .028$, d = 0.359, suggesting a generally alerting effect of odorant stimulation.

To support the assumption of a generally altering effect of the odorant stimulation (see discussion), we additionally compared the correct responses between the control conditions for the mid speaker positions. This data-driven analysis confirmed that birhinal stimulation ($M = 93.50\%$, $SD = 6.70\%$) also had an enhancing effect on the localization performance compared to an auditory-only control condition ($M = 90.51\%$, $SD = 6.93\%$), $t(140.015) = 3.937$, $p < .001$, d = 0.566.

Response times for lateral sounds are not affected by odorant stimulation

In contrast to the proportion of correct responses, reaction times for lateralized sounds were only marginally affected by the manipulated factors. Mainly, participants responded faster to sounds at far-out ($M = 369.787$ ms, $SD = 52.16$ ms) compared to mid-out ($M = 396.423$, $SD = 55.50$ ms) sound positions. Apart from this main effect of *sound position*, $F(1,24) = 142.282$, $p < .001$, $\eta_p^2 = 0.856$, no further effects reached significance (all $p \geq .084$).

Note that all results remained unchanged when strongly biased participants were excluded from the analysis.

2.2 EEG Results

2.2.1 Univariate analysis of alpha power lateralization

Alpha power lateralization in response to central sounds confirms that participants allocate attention to the chosen sound location, but remains insensitive to condition differences

Figure 2 (B-D) depicts the alpha lateralization index (ALI) for each stimulation condition (auditory-only, birhinal, congruent, incongruent) as a function of sound position (far-out vs. mid-out vs. central). For centrally presented sounds, the alpha lateralization index is computed relative to the given response such that congruency between odor-stimulation and perceived or chosen sound location is reflected. A cluster-corrected sign-permutation test showed a small, but significant ($p = .0395$) overall lateralization of alpha power in-between ~320 to 650 ms post-stimulus onset, indicative of a spatial shift of attention towards the selected hemifield. However, a rmANOVA of average alpha lateralization magnitude (revealed no significant differences between the stimulation conditions, $F(2.06, 49.34) = 0.225$, $p = .805$, $\eta_p^2 = 0.009$, after Greenhouse-Geisser correction ($\varepsilon = 0.69$).

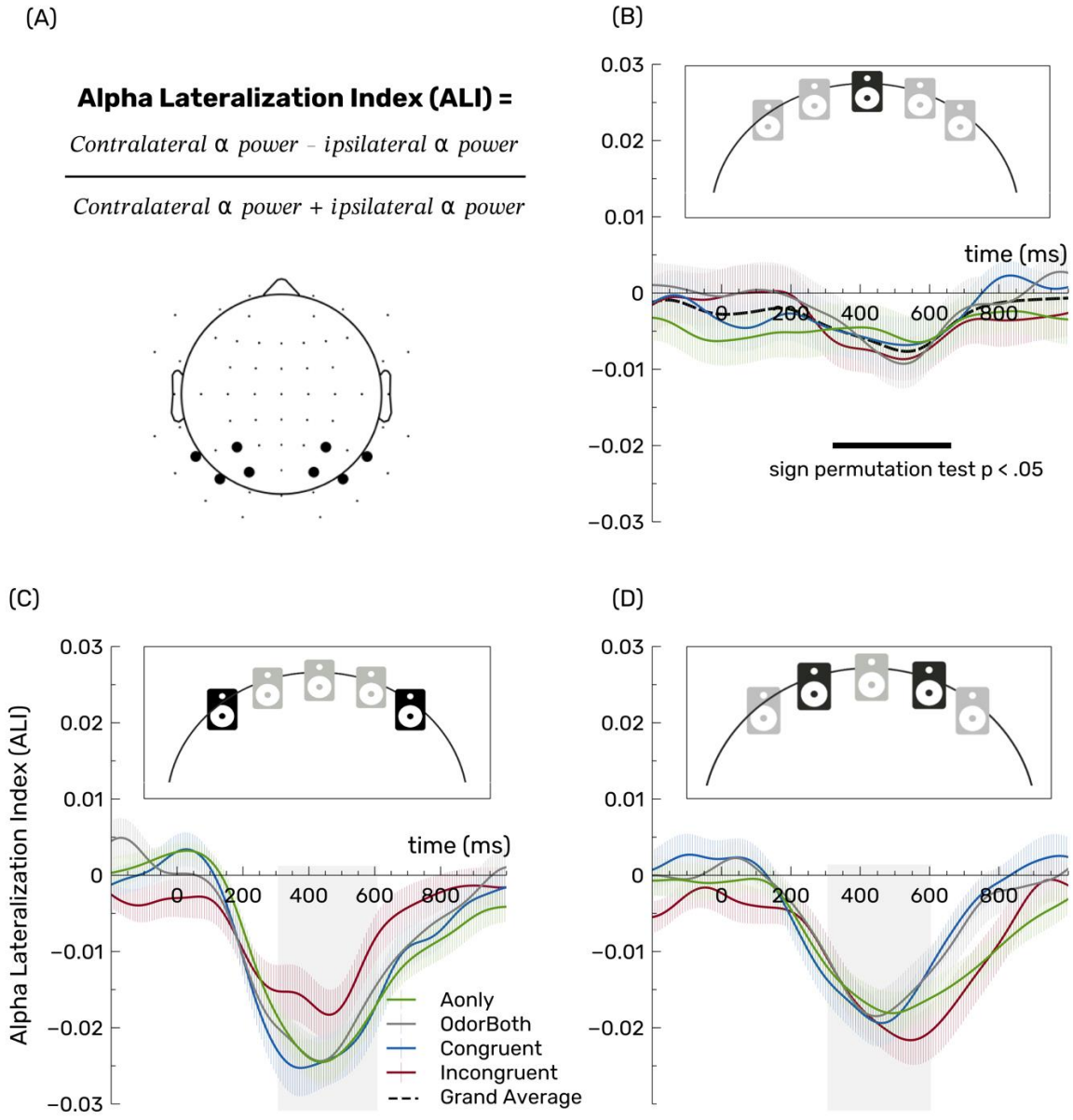

Figure 2. Magnitude of alpha lateralization is modulated by congruency between chemosensory and auditory spatial information, but only when disparity between the senses is high. (A) Alpha power (8-12 Hz) lateralization was expressed in terms of a normalized hemispheric difference between contralateral and ipsilateral electrode sites Panels (B)-(D) depict the time course of alpha power lateralization per condition for sounds presented at central (B), far-out (C), and mid-out (C) positions, respectively. In the former case, contralateral and ipsilateral alpha power was computed relative to the chosen response category (right vs. left) instead of the physical sound position.

Alpha power lateralization in response to lateral sounds indicates a disruption of spatial attention when disparity between auditory and chemosensory cues is strong

A two-way rmANOVA revealed no significant main effect of *stimulation*, $F(3,72) = 0.799$, $p = .498$, , $\eta_p^2 = 0.032$. In contrast, a significant main effect of *sound position* was evident, $F(1,24) = 6.976$, $p = .014$, $\eta_p^2 = 0.225$, in addition to a significant interaction of *stimulation* and *sound position*, $F(3,72) = 3.434$, $p = .021$, $\eta_p^2 = 0.125$. Follow-up paired-sample *t*-tests showed that no

significant differences between conditions were obtained at lateralized positions close to midline (mid-out; all $p \geq .45$), while alpha power lateralization was significantly modulated by odor-stimulation at strongly lateralized (far-out) sound positions. Specifically, incongruent odorant stimulation (M = -0.015, SD = 0.0149) resulted in a reduction of alpha power lateralization compared to congruent stimulation (M = -0.023, SD = 0.0169), $t(24)$ = -3.0827, p = .0051, p_{corr} = 0.0378, d = -0.617. Alpha power lateralization in incongruent trials was further significantly reduced compared to the auditory-only condition (M = -0.022, SD = 0.011), $t(24)$ = 2.9165, p = .0076, p_{corr} = 0.0378, d = 0.583, as well as birhinal stimulation (M = -0.021, SD = 0.016), $t(24)$ = 2.4122, p = .024, p_{corr} = 0.080, d = 0.482; albeit, please note that the latter comparison did not remain significant after correction for multiple comparisons. The magnitude of alpha power lateralization at far-out sound positions and in congruent trials did not differ significantly from the control conditions with birhinal stimulation $t(24)$ = -0.8104, p = .426, p_{corr} = .715, d = -0.162, or auditory-only stimulation, $t(24)$ = -0.5731, p = .5719, p_{corr} = .715, d = -0.115. A supplementary analysis, including the additional factor *sequence half,* confirmed the two-way interaction between sound position and condition, $F(3,72)$ = 2.904, p = .041, η_p^2= 0.108, while the three-way interaction of *sound position, condition, and sequence half* was not significant, $F(3, 72)$ = 1.323, p = .274, η_p^2= 0.052 (see supplementary section S1).

2.2.2 Multivariate pattern analysis

Decoding accuracy decreases with concurrent odorant stimulation, but remained insensitive to the differences between odorant-stimulation conditions

To fully exploit the multivariate nature of EEG, we decoded the spatial location of a sound (i.e., left vs. right) based on the topography of alpha-band power (for a schematic illustration of the procedure, see Figure 3-A). Figure 3-B, C, and D depict the time-course of decoding accuracy as well as average decoding ability, separately for the four stimulation conditions, respectively. Generally, the time course follows a similar trajectory across conditions. Decoding accuracy starts to rise above chance level as early as ~160 ms after sound onset, reaches its peak at around ~480 ms, and then gradually declines towards the end of the trial. The cluster-based permutation procedure yielded a sustained cluster of significant decoding accuracy for auditory-only trials ($p < 10^{-4}$, 162 – 995 ms), bilateral odor-stimulation ($p < 10^{-4}$, 256 – 995 ms), as well as congruent ($p < 10^{-4}$, 170 ms – 995 ms) and incongruent ($p < 10^{-4}$, 199 – 995 ms) odorant stimulation. Pairwise comparisons of the time course of decoding accuracy between conditions, using a cluster-corrected sign-permutation test, showed that decoding accuracy was consistently higher in auditory-only trials in comparison to trials with incongruent odorant stimulation (p = .0227, 235 – 445 ms), trials with congruent odorant stimulation (p = .0374, 264 – 517 ms), and trials with bilateral odorant stimulation (p < .001, 170 – 676). There were no significant differences in the time course of decoding accuracy between the three odorant-stimulation conditions (all p > .190). A follow-up analysis, contrasting average decoding ability between 338 and 638 ms following sound onset substantiated these results (Figure 3-D), showing higher average decoding ability for auditory-only stimulation relative to birhinal stimulation (p < .001), congruent (p = .0076), and incongruent stimulation (p = .0040; all other p ≥ .62).

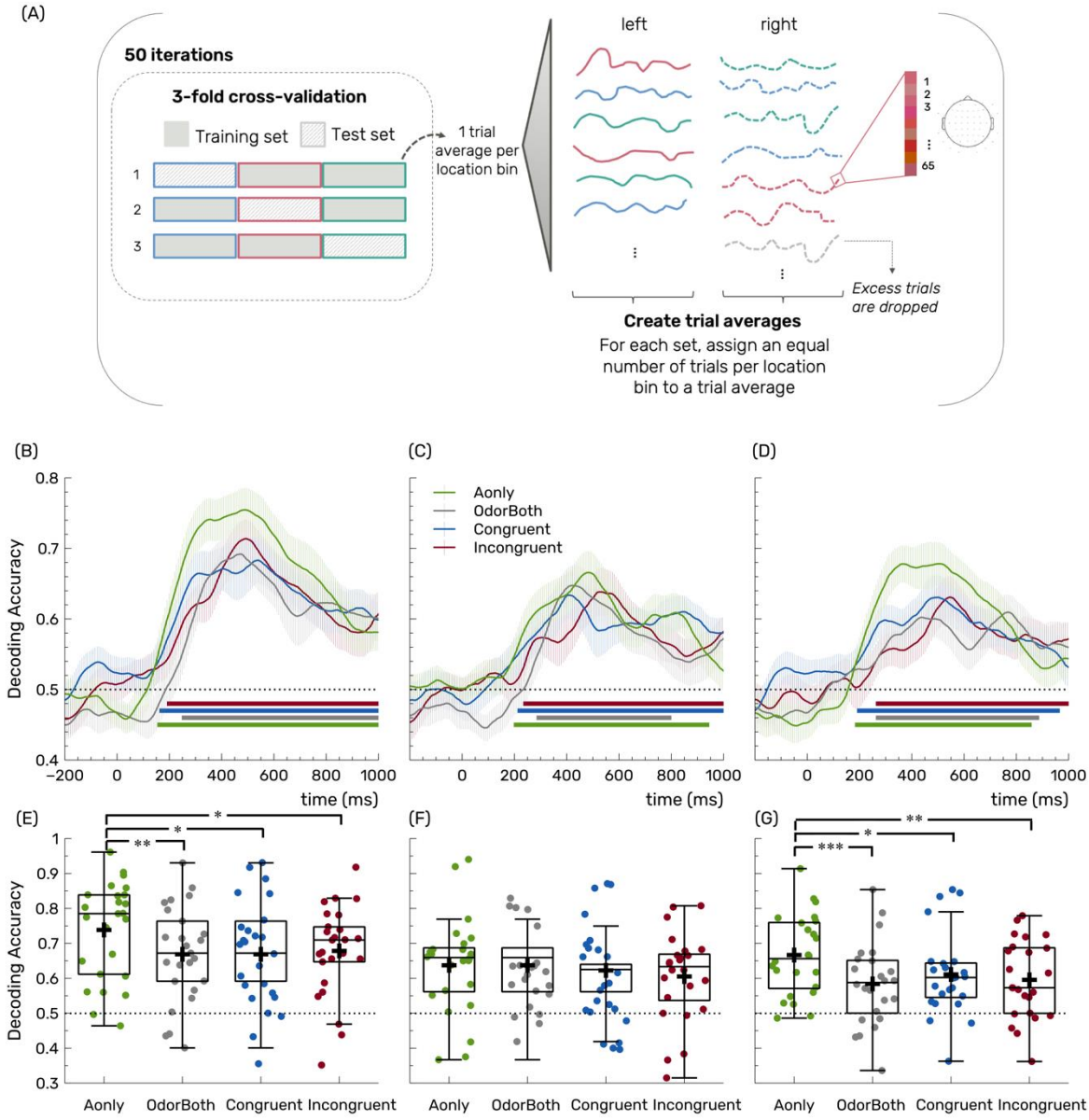

Figure 3. Decoding accuracy is generally diminished by concurrent odorant stimulation, but this remains insensitive to the congruency between chemosensory and auditory spatial information. (A) Schematic figure of the applied train- and test-classification procedure. Panel (B) depicts the time course of decoding accuracy in the four conditions, based on all trials with lateralized sound presentation. In addition, to differentiate between immediate and after-effects of odorant stimulation, the decoding analysis was run separately for trials in the first (C) versus second (D) half of the sound sequence. Boxplots in panels (E), (F) and (G) depict the average decoding accuracy per condition for all trials and trials in the first or second half of the sequence, respectively. Scattered dots correspond to the average decoding accuracy per subject. Lines in the boxplots indicate the median whereas the plus indicates the mean, and whiskers denote +-1.5 IQR Average decoding accuracy between conditions was contrasted using a two-sided permutation test. Significant comparisons are denoted with * (p < .05), ** (p < .01), or *** (p < .001).

In line with an after-effect of stimulation, drop in decoding accuracy with concurrent odorant stimulation is exclusively present in the second half of the sound sequence

To further assess whether the effects of odorant stimulation result from the immediate stimulation or present an after-effect of the stimulation, we performed two separate decoding analyses including trials from the first half of the sound sequence (immediately paired with odor-stimulation) and trials from the second half of the sound sequence (after-effect of odor-stimulation). Decoding ability remained significantly above chance in all conditions (all $p < 10^{-4}$). Critically, in line with the behavioral results, showing that sound localization performance was predominantly modulated by after-effects of odor-stimulation, the drop in decoding ability with concurrent odorant stimulation was only present in the second half of the sound sequence (see Figure 3 C vs. D and F vs. G). Accordingly, a cluster-corrected sign-permutation test, yielded no significant differences in the time-course of decoding ability between conditions (all $p > .423$) in the first half of the sequence. In contrast, during the second half of the sequence, decoding accuracy for auditory only trials significantly exceeded decoding accuracy of trials with incongruent ($p = .0028$, 235 – 481 ms) as well as bilateral odorant stimulation ($p < .001$, 213 – 654 ms; all other pairwise contrasts n.s., all $p \geq .143$). Contrasting the average decoding ability (first sequence half: 316 - 616 ms, second sequence half: 360 – 660 ms) between conditions, yielded no significant differences between condition during the first half of the sequence (all $p \geq .223$). However, substantiating, the time-resolved comparisons, average decoding ability for auditory-only trials was higher compared to the average decoding ability in trials with birhinal odorant stimulation ($p < .001$), with congruent odorant stimulation ($p = .0218$), and compared to incongruent odorant stimulation ($p = .004$).

3. Discussion

Sound localization is biased towards lateralized trigeminally potent chemosensory cues when sound cues are highly ambiguous

Receiving conflicting input through different sensory channels poses a unique challenge for the brain. Here, we investigated to what extend a task-irrelevant, yet highly salient (i.e., trigeminally potent) bimodal odorant may affect sound localization judgements. In line with a previous report of an odorant-induced sound localization bias[5], we find that the proportion of centrally presented sounds that was categorized as coming from the right increased with right-nostril odorant stimulation, while it decreased with left-nostril stimulation (compared to two control conditions with birhinal nostril and auditory-only stimulation, respectively). On the electrophysiological level, this effect was accompanied by a significant lateralization of parieto-occipital alpha power, signifying the allocation of auditory spatial attention[13,19,22,37,38] towards the hemifield where the sound was localized. This finding is critical to verify that the present design, where participants were unaware of the central loudspeaker, while performing a forced-choice localization judgement, was effective in eliciting a shift of spatial attention towards the perceived (rather than the physical) sound location.

Notably, the odorant-induced localization bias was only consistently present in trials during the second half of the sound sequence, speaking in favor of an after-effect as opposed to an immediate effect of odorant stimulation. This is in line with the notion that chemosensory

processing is considered to be relatively slow compared to other sensory modalities. For instance, the chemosensory P3 component, elicited by trigeminally potent odorants, is known to occur after 800 – 1300 ms[39] as compared to after ~300 ms in typical visual paradigms [40]. In addition, trigeminally potent concentrations of bimodal odorants evoke peak magnitude neuronal responses in the mouse piriform cortex after ~1s post-stimulus offset that persist thereafter until up to 3 s[41]. Furthermore, in human subjects, it has been shown that that brief (i.e., 200 ms) trigeminally potent stimulation in high concentrations evokes stinging perceptions at 2 s post-stimulus, reaching their maximum at around 4.5 s, and lasting up to 11 s post-stimulus onset[42]. Perceptions of relatively lower concentrations were further delayed, starting at 5 s post-stimulus, reaching their maximum at around 10 s, and lasting up to 20 s post-stimulus onset. These slower burning perceptions are due to the involvement of unmyelinated C-fibers, as opposed to myelinated A δ -fibers that are responsible for the faster stinging perceptions[35,36]. In the current experiment, we used concentrations that were slightly above the lateralization threshold, thus might have predominantly involved C-fibers and evoked slower burning perceptions, thus aligning rather with the second half of the sound sequence.

In contrast to the effect observed for centrally presented sounds, the effect of odorant stimulation became spatially unspecific with increasing discernability of the sound cues (i.e., at +/- 5° azimuth). That is, the participants showed better performance in all odorant conditions compared to an auditory-only control condition, irrespective of whether the nostril-side was congruent or incongruent with the actual sound location. This suggests a more general alerting function, potentially driven by the unpleasant sensation of the trigeminal component. Notably, though, when sounds were most strongly lateralized and hence, clearly discernable in terms of their spatial position (at +/- 15° azimuth), performance was close to ceiling in all conditions and there was no effect of odorant-stimulation. Overall, this pattern is in line with the notion that chemosensory cues exert an effect on perception in other modalities only when the latter is ambiguous. Accordingly, Zhou and Chen[43] found that fearful sweat biased female participants toward rating ambiguous facial expressions as more fearful, while the same odorants had no effect when the facial expression was more apparent. On a similar note, Zhou and colleagues[44] reported an effect of olfactory cues on binocular rivalry, a form of multistable perception caused by the presentation of dissimilar images to the two eyes[45]. While these previous studies concern cross-modal interactions between vision and olfaction, the present study extends those findings to chemosensory and auditory perception.

A common attentional control system for auditory and chemosensory processing?

The results can also be regarded in light of a common attentional control system that governs the integration of unimodal spatial representations, as it has been suggested for other sensory modalities such as vision and touch[46] or vision and chemosensation[47]. According to such a notion, the brain attempts to integrate spatial cues into a common spatial reference frame. Consistent with the idea of common spatial representation, Frasnelli and colleagues[48] provide fMRI evidence showing that the localization of bimodal odorants shares dorsal processing stream with other sensory modalities. Specifically, they found that presentation of bimodal odorants, stimulating both the olfactory as well the trigeminal system, also activated the intraparietal sulcus and superior temporal sulcus, both of which present areas previously

associated with multisensory integration[49,50]. The former has also been shown to be activated when localizing auditory stimuli[51,52]. The above framework[46] is clearly suggestive of a link between spatial attention and multisensory integration. In the present study, this is especially apparent, when auditory spatial cues were highly unreliable (i.e., sounds were presented from a central position) and thus, trigeminally delivered spatial information had to be taken into account to derive a localization decision. This resonates well with the proposal that resolving sensory ambiguities present a major function of multisensory integration[53].

On the contrary, our results show that the deployment of spatial attention was only disrupted when the discrepancy between the sound location and the chemosensory cues was largest – that is, when the sound was presented at one of the outmost locations (+/-15° azimuth) and the opposite nostril was stimulation. Such maximally incongruent stimulation resulted in a diminished lateralization of alpha-band power. However, this disruption of attentional allocation was not sufficiently strong to be reflected on the behavioral level, where performance was close to ceiling in all conditions. This does not necessarily disprove a common attentional control system. It remains possible that a common or supramodal attentional system weighs input from different system modalities. However, it should be noted that albeit the fact that alpha power lateralization is frequently linked to a supramodal attentional mechanism[23,37,54,55], compelling evidence for such a notion remains scarce. Irrespective of this debate, our results clearly demonstrate that alpha power lateralization is susceptible to cross-modal input from the chemosensory domain.

The present results are also interesting in light of a line of research that has investigated the effect of trigeminally potent olfactory cues in spatial cueing paradigms[56–58]. Those studies adopt an exogenous cueing approach, in which the lateralized odorants are non-predictive of the targets and thus, similar to the present study, task-irrelevant. Wudarczyk and colleagues[58] report a small but significant facilitation of visual target detection by congruent trigeminal cues. Albeit only evident after repeated exposure to the trigeminal cues, the findings generally corroborate the notion that a shared attentional mechanism could be captured by task-irrelevant trigeminal cues. On the contrary, another study[57] found no cueing effect for mixed olfactory-trigeminal cues, but rather a general acceleration of response times for all types of odorant cues. Nevertheless, the results do align well with our findings. First of all, our findings clearly show that trigeminal cues seem to only exert a clear effect on behavioral judgements in another modality, when auditory cues provide little to no spatial information. In classical spatial cueing studies this is not the case (i.e., the stimuli in the task-relevant modality are clearly lateralized), resulting in only weak effects after repeated exposure[58] or spatially-unspecific arousal effects [57]. The latter is consistent with our findings for mid-out sounds, although in the present study the effect was reflected in accuracy rather than response times. Secondly, temporal factors seem to play a critical role for chemosensory stimulation to exert its effect[56]. Our results clearly show that odorant-induced bias is largely driven by an after-effect of odorant stimulation, emphasizing that cross-modal interactions involving the chemosensory domain take time to evolve. That said, the present paradigm, using a prolonged odorant stimulation interval (i.e., 4 s) as well as an equally long post-stimulation period, may be more optimally suited to capture such interactions as compared to a classical cueing paradigm, in

which stimulus-onset-asynchronies range in-between ~500 and ~1000 ms and odorant stimulation is typically shorter (i.e., ~500 – ~1000 ms).

Cross-modal interactions are reflected in posterior alpha lateralization but not in multivariate decoding of the alpha band topography

To capture cross-modal interactions between audition and chemosensory processing, the present study focused on attentional modulations of alpha-band power. In line with previous work[23,59], we were able to decode the locus of covert auditory attention based on the topography of alpha-band power. However, decoding accuracy was insensitive to spatial information provided via chemosensory cues. Albeit there was a general reduction in decoding ability with concurrent odorant stimulation compared to auditory-only trials, decoding accuracy did not differentiate between congruent and incongruent odorant stimulation. While previous studies found a multivariate decoding approach to be more sensitive to experimental manipulations of spatial attention as compared to a classical univariate measure[59], this was not the case in the present study. Previous work has shown that spatial information derived from chemosensory cues is predominately encoded in the delta frequency range[60]. Hence, considering other frequency bands outside of the alpha-range might present a worthwhile opportunity for future studies.

However, the univariate analysis of hemispheric differences in alpha-band power clearly showed that the coding of auditory spatial information in alpha oscillations is generally susceptible to conflict spatial information in another modality. As discussed above, our results show that magnitude of alpha power lateralization was modulated by a strong disparity of spatial information provided by the two senses. But what stands out is the fact that when the auditory cues were maximally ambiguous with respect to spatial information (i.e., in trials with centrally presented sounds), the magnitude of alpha power lateralization did not differentiate between the different odorant-conditions. This seems somewhat at odds with the behavioral results. In accordance with the latter, we expected a congruent odorant to boost and an incongruent odorant to diminish the magnitude of alpha power lateralization. Yet, considering that the overall effect of alpha lateralization in response to central sounds was very small, this leaves very little room for condition-specific differences to emerge. Several factors may have contributed to the overall rather small effect. Most importantly, participants had to make a forced choice between left versus right. Hence, the trial averages may include trials in which the chemosensory cues did successfully capture attention, but also trials in which they did not. In future studies it might be worth including a central response option to more clearly differentiate between illusion and no-illusion trials[2,61]. Further, the range of spatial locations in the present study was limited and apart from the central sounds, all lateralized sounds were presented at locations that fall well in the range of clearly localizable positions. Considering the remarkable ability of our auditory system to detect even small deviations from a central position (i.e., as little as 1° [62]), future studies should include sound positions closer to midline and consider a continuous response format.

Limitations and open questions

Rather unexpectedly, we found that the even in the two control conditions (auditory-only, birhinal), the proportion of right- and left-responses to the centrally presented sounds was not

equally distributed. Instead, most participants showed a clear preference towards categorizing the central sounds as coming from the left or right side. In a spatial cueing study with olfactory cues[63], responses were generally faster for right targets. The authors proposed that this might present a side effect resulting from lateralization processes due to all responses being conducted with the right hand. This explanation does not fully align with our data. Participants always responded with their dominant hand. But neither were the two left-handed subjects among the participants with a strong left-ward bias (i.e., > 90% left-ward responses in the control condition), nor does the number of left-handed participants match the number of participants showing a left-ward bias. We speculate that the high degree of uncertainty for the centrally presented sounds led to participants choosing a preferred side. Critically, the observed odorant-induced sound localization bias occurred irrespective of this general response-side-preference.

Since previous studies have consistently shown that the trigeminal component is required to consciously localize olfactory cues, it is most likely that the present effects are driven by the trigeminal component. However, it should also be noted that some studies provide evidence for an implicit effect of spatial olfactory cues below the trigeminal threshold[63], proposing a residual ability of directional smelling based on purely olfactory cues. Here, we did not include a respective control condition with a purely olfactory stimulus, as the original study by Liang et al[5] showed no sound localization bias when using phenylethyl alcohol as an odorant.

Further, an important aspect of the present design to take into consideration concerns the lack of any natural association between the stimuli presented in both modalities. An interesting avenue for future research could be to explore to what extent the use of environmental stimuli, giving rise to semantic (in-)congruency could boost or diminish the present effects. Kuang and colleagues[3] provide an interesting example of how a learned association between naturally occurring odorants (e.g., banana smell) and motion directions can bias the perception of ambiguous moving dot patterns.

Conclusion

Taken together, the present study corroborates evidence for a spatial ventriloquism effect between the auditory and the chemosensory domain and demonstrates, for the first time, how this is reflected in electrophysiological correlates of spatial attention. Collectively, the present study lays fundamental groundwork to advance our understanding of cross-modal interactions between chemosensory and auditory processing and points out promising avenues for future research.

4. Methods

4.1 Power Analysis

We conducted an a-priori power analysis, using MorePower 6.0[64]. Liang et al.[5] reported an effect of right-nostril menthol stimulation on the proportion of right-ward responses for sounds at azimuth = 0° compared to a control condition (d = 0.608, i.e., η_p^2 = 0.2752). Accordingly, aiming for a power of 80% and an effect size of interested of η_p^2 = 0.275 in a paired-sample t-test, the power analysis yields a required sample size of n = 24.

4.2 Sample

A total of 32 participants were recruited for this study. A subset of 8 participants took part as part of a practical EEG seminar, taught at the Ruhr University Bochum in the summer semester of 2023. Exclusion criteria entailed migraine, pregnancy, history of neurological or psychiatric diseases, asthma, acute or chronic upper airway diseases, acute allergies affecting the respiratory system, current influence of a drug, alcohol, or a controlled substance, impaired hearing ability or olfaction, as well as a hairstyle incompatible with EEG recordings. Hearing levels of all participants were assessed by means of a pure tone audiometry (Oscilla USB 330; Immedico, Lystrup, Denmark). The fully automated procedure included the presentation of eleven pure tones at varying frequencies (i.e., 125 Hz, 250 Hz, 500 Hz, 750 Hz, 1000 Hz, 1500 Hz, 2000 Hz, 3000 Hz, 4000 Hz, 6000 Hz, 8000 Hz). In addition, on the day of the experiment, participants were required to pass a pulmonary lung function following to the ATS/ERS 2019 spirometry standards [65], that is, forced exhaled volume (FEV1) must surpass 85% (Vyaire Sentry Suite). Moreover, an olfactory function test (Sniffin' Sticks identification subtest, Burghart Messtechnik GmbH, Wedel, Germany; Hummel et al., 2007; Oleszkiewicz et al., 2019). In addition, the nasal flow rate of both nostrils was examined by means of an active anterior rhinomanometry (RHINO-SYS, Happersberger otopront GmbH, Hohenstein, Germany) to determine if participants showed signs of a nasal flow asymmetry.

Three participants were excluded because the odorant lateralization paradigm (see section 4.4.1) had to be aborted prior to reaching the required performance level. Further, two participants were excluded due to insufficient lung function (spirometry, forced exhaled volume < 85%). In addition, one participant was not able to properly execute the velopharyngeal closure technique, while another participant was excluded for the intake of psychotropic drugs. That is, the final sample included 25 participants (male = 12, female =13).

The mean age in the sample was 24.8 years (*SD* = 3.52). 23 participants reported to be right-handed, two participants were left-handed. The majority of participants (*n* = 20) indicated to be non-smokers, 4 participants indicated to smoke only occasionally, while 1 participant indicated that they smoked on a regular basis. Note that smoking did not result in exclusion, as long as participants passed the odorant lateralization paradigm, as described in section 4.4.1. Due to a technical error, audiometry data for two subjects were not saved. Considering all other subjects in the sample, hearing thresholds for all tested frequencies were ≤ 25 dB in 22 subjects, indicating unimpaired hearing [68]. Four subjects showed negligible outliers at 30 dB (n = 3) and 35 dB (n = 1) for one of the tested frequencies, while all other frequencies fell below 30 dB. Since the stimuli used in the present study were broad-band (see section 4.3), those outliers were considered negligible. The average forced exhaled volume in the sample was 101.04% (*SD* = 10.19). On the Sniffin' Sticks olfactory function test, participants scored on average 12.13 out of 16 points (*SD* = 1.72). The flow data of the two nostrils did not differ significantly as controlled using paired *t*-tests, neither for the influx, $t(22) = 1.26$, $p = .22$, nor for the efflux, $t(22) = 1.35$, $p = .19$. Thus, there was no systematic bias with respect to the stimulated nostril. All participants provided informed consent prior to the beginning of the experimental procedure. The study was approved by the local ethics committee at the Leibniz Research Centre for Working Environment and Human factors and conducted in accordance with the

Declaration of Helsinki. As compensation for their time, participants received 12 Euros per hour (or course credit).

4.3 Apparatus and stimuli

The experiment took place in a dimly lit, sound attenuated room (5.0 × 3.3 × 2.4 m) with pyramid-shaped foam panels on ceiling and walls and a woolen carpet on the floor to dampen the background noise level (i.e., below 20 dB(A)). The experiment was programmed and controlled using ePrime 3.0 (Psychology Software Tools, Pittsburgh, PA) on a Windows 10 computer. The synchronization of auditory stimuli and EEG triggers was controlled using an AudioFile Stimulus Processor (Cambridge Research Systems, Rochester, UK). Participants were seated in a comfortable chair at a distance of approximately 130 cm from a 49'' centrally aligned 1800R curved monitor (5120 x 1440 pixel resolution, 100 Hz refresh rate, Samsung, Seoul, South Korea), while placing their head on a chin rest that prevents head movements during the experiment. Below the screen, five full-range loudspeakers (SC 55.9 –8 Ohm; Visaton, Haan, Germany) were mounted at -15°, -5°, 0°, +5°, and +15° horizontal azimuth (Figure 1-B). Loudspeaker locations at -5° and +5° are also referred to as "mid-out positions", whereas the loudspeaker locations at -15° and +15° are referred to as "far-out positions". To prevent participants from knowing the exact loudspeaker positions, the loudspeakers were covered by an opaque, sound-permeable curtain. Critically, the participants were not aware of the presence of the central loudspeaker. As auditory stimuli, a 250 ms broad-band pink noise was generated. All sound stimuli were presented at a sound level of ~61 dB(A). Isopropanol, dissolved in water at an individualized concentration (ranging from 50% - 75%) was used as a bimodal odorant substance. Isopropanol is a commercially available substance which is used amongst others in making cosmetics, skin or hair products, perfumes, and disinfectants. The intranasal stimulation with isopropanol can evoke unpleasant odor- or gustatory perceptions. Additionally, the trigeminal component of the bimodal odorant elicits an immediate short-lasting irritating sensation in most subjects [69,70]. For olfactory stimulus presentation, an EEG-compatible computer-controlled flow-olfactometer with a constant air flow of 2.5 l/min (NeuroDevice, Version 2, Warsaw, Poland) was used. For an elaborate description of the device and for technical adaptions made in order to optimize the setup for concurrent EEG recordings, please see Hucke et al., (2018, 2021), respectively. Briefly, the olfactometer delivers olfactory stimuli into the participants nostrils via a nasal cannula. To allow for monorhinal odorant stimulation, a custom-built clip separates the two nasal tubes, however, birhinal stimulation is possible as well. The olfactometer integrated the odorous stimulus into the constant air flow of clean air and thereby ensures a seamless and precise stimulus on- and offset. This mechanism spares a potential co-activation of mechanoreceptors of the trigeminal nerve.

4.4 Procedure and experimental protocols

Prior to the experiment, participants were informed about the experimental procedure and the potentially irritating effects of the stimulation with isopropanol. First, all participants were screened for exclusion and inclusion criteria and the required pre-assessments were conducted. The latter included a pulmonary lung function (spirometry), the Sniffin' Sticks olfaction test, a rhinomanometry, as well as a pure tone audiometry. Note that in the educational sample (n = 8), only the spirometry was strictly required to take place prior to the

EEG recording. Afterwards, participants were prepared for the EEG recording and instructed to practice the velopharyngeal closure technique. The latter refers to a breathing technique that aims to seal the velum and pharyngeal walls and prevent air flow from the oral to the nasal cavities while breathing through the mouth (Kobal, 1981). This ensures that olfactory stimulation is not affected by the participant's respiration. To ensure trigeminal involvement, first, participants' odorant lateralization threshold is determined (as described in section 4.4.1). Once the final concentration is determined, participants continue with the sound localization task (as described in section 4.4.2). The entire experimental procedure (including EEG cap preparation) took approximately 2 - 2 ½ hours.

4.4.1 Odorant lateralization paradigm

To ensure that all participants were able to report the location of the bimodal olfactory stimulus, a lateralization paradigm was conducted (Figure 1-A). The latter comprised an iterative procedure in which participants were asked to indicate the location of an monorhinally-presented bimodal odor stimulus as left vs. right. All participants started with a concentration of 50% isopropanol. Odorant stimulation occurred randomly in the left or right nostril for 4 seconds and was followed by a stimulation-free inter-trial interval of 10 seconds (plus a random jitter of 0-100 ms). To make sure that participants' attention was focused at the beginning of each trial, despite the long inter-trial interval, the fixation cross briefly increased in size 1000 ms prior to odorant stimulation onset to signal participants to anticipate the next odorant stimulus. If participants did not reach a localization accuracy of at least 80% in a block of 20 trials, the concentration was increased by 5%. To pass the lateralization test, accuracy had to be at least 80% on average in two consecutive blocks with the same isopropanol concentration. In the final sample, the median isopropanol concentration was 50% (range = 50-75%).

4.4.2 Sound localization paradigm

A schematic trial sequence of the sound localization paradigm is depicted in Figure 1-C. The sounds are grouped into sequences of 8 tones with an inter-stimulus-interval of 950 ms (+ 0-100 ms random jitter). This amounts to roughly 8 s for a sound sequence. In the analysis, we will differentiate between sounds in the first (sounds 1-4) as opposed to the second half (sounds 5-8) of the sequence. The participants are asked to indicate the perceived direction (left vs. right) of each sound in a sequence. Participants respond via button press using the index and middle finger of the dominant hand. They are informed that some sounds will be easier, others very hard to localize. A total of eight sequences constitutes one block. Each block can be assigned to one of the following conditions: (i) auditory-only, (ii) birhinal, (iii) monorhinally left, or (iv) right isopropanol stimulation using a flow-olfactometer (NeuroDevice, v2). Each odorant sequence contains a respective odorant stimulation for 4 s that is time-locked to the first sound in the sequence (Figure 1-D). Due to the rising time of the olfactometer and the molecules build-up in the nasal mucus it is expected that the odorant perception roughly overlaps with the entire sound sequence. In blocks including form of odorant stimulation, the inter-sequence-interval was 13.6 s to minimize habituation or sensitization. In auditory-only blocks, the inter-sequence-interval was reduced to 3 s. 1000 ms prior to the first stimulus presentation in a sequence, the fixation briefly increased in size to signal the beginning of the

next sound sequence. Participants completed a total of 8 auditory-only blocks, and 12 odor-blocks in a randomized order. After 4 blocks, participants were invited to take a self-paced break. The order of sound locations within a sequence is counterbalanced and pseudo-randomized across the all trials of the experiment and conditions (auditory-only, birhinal, odor-left, odor-right) such that 50% of all sound stimuli were presented at 0° azimuth and in 12.5% of cases at each lateralized position (+/- 15°, +/- 5°).). This was motivated by the fact that the main (behavioral analysis) focuses on the localization of sounds at the central position. For details on how the trials are sorted into the conditions, please refer to Table 1. Participants were presented with 5 practice auditory-only sequences to familiarize themselves with the sequence structure and pace. Participants were instructed to breathe through their mouth while performing the velopharyngeal closure technique throughout the experiment. Since some participants reported difficulties to continuously apply the breathing technique, they were allowed to normally breathe through their mouth in the inter-sequence interval, when no sound or odorant-stimulation was present. Further, to dampen discomfort due to dry mouth feel, participants were encouraged to drink water and switch to nasal breathing during the breaks.

4.5 EEG data acquisition

The electroencephalogram was recorded using 64 Ag/AgCl electrodes (BrainCap, Brainvision, Gilching, Germany) and digitized with a 1000 Hz sampling rate, using a NeurOne Tesla amplifier (Bittium Biosignals Ltd, Kuopio, Finnland). The electrode arrangement across the scalp was in accordance with the extended international 10-20 system. AFz and FCz served as the online ground and reference electrode, respectively. During cap preparation, electrode impedances below 20 kΩ were ensured.

Table 1. Trial numbers split according to the sound locations (5 speaker) and stimulation (auditory-only, odorant-birhinal, odorant-left, odorant-right) and the respective sums across the locations and conditions.

	Sound location					
Condition	Far-left (-15°)	Mid-left (-5°)	Central (0°)	Mid-right (+5°)	Far-right (+15°)	Sum condition
Auditory-only	64	64	256	64	64	512
Odorant-birhinal	32	32	128	32	32	256
Odorant-left	32	32	128	32	32	256
Odorant-right	32	32	128	32	32	256
Sum location	160	160	640	160	160	**Total: 1280**

4.6 EEG preprocessing

The raw EEG data was preprocessed and cleaned from artifacts using a customized, automated preprocessing pipeline, implemented in MATLAB (R2021b and R2023a) and EEGLAB (2021.1[74]). First, a non-causal, zero-phase Hamming windowed sinc FIR high-pass (pass-band edge: 0.01

Hz, transition band width: 0.01 Hz, filter order: 330000, -6dB cutoff frequency: 0.005 Hz) and low-pass filter (pass-band edge: 40 Hz, transition band width: 10 Hz, filter order: 33, -6dB cutoff frequency: 45 Hz) were applied to the continuous data. Then, electrodes compromised by artifacts were identified based on statistical properties of the data. That is, using the built-in EEGLAB function *pop_rejchan(),* electrodes with a normalized kurtosis value exceeding 5 standard deviations of the mean were identified and excluded. Prior to normalization, the distribution of kurtosis values was trimmed, removing the highest and lowest 10% of values. In addition, any electrodes with periods of flatline recordings of more than 5 seconds were removed using the function *clean_flatlines*() with default parameters. On average, 4.48 electrodes were removed per subject (*SD* = 1.69). To restore the data at previously removed electrodes, a superfast spherical interpolation algorithm was applied, using the built-in EEGLAB function *pop_interp()*. In a next step, the data was re-referenced to the average of all channels, while retaining the original reference channel FCz in the dataset. At this point, two copies of the dataset are created. The first copy (in the following also referred to as the reference dataset) will be resumed at a later time point. The second copy is submitted to an ICA-based artefact identification procedure, consisting of the following steps: First, to speed-up and optimize ICA, a copy of the dataset was down sampled to 200 Hz and high-pass filtered at 1 Hz (pass-band edge, transition band width: 1 Hz, filter order: 3300, -6dB cutoff frequency: 0.5 Hz). The latter has been shown to increase the percentage of 'near-dipolar' independent components (ICs; [75]). Then, the data was segmented into epochs ranging from -1500 ms to 1500 ms relative to each sound onset and submitted to an automated trial-rejection procedure (i.e., *pop_autorej()*). The latter is implemented in two steps: first, trials with unreasonably large amplitude fluctuations (i.e., > 1000 μV) are removed. Second, an iterative algorithm rejects epochs containing data values outside a standard deviation (*SD*) threshold of ± 5%. On each iteration, a maximum of 5% of all trials can be rejected. If the number of epochs marked for rejection exceeds this limit, the *SD* threshold is increased by 0.5 *SD* and the next iteration is performed. When no more data epochs are identified with the current *SD* threshold, the threshold is lowered again by 0.5 *SD* and the iteration continues until either no more epochs are identified for rejection or until a maximum number of eight iterations has been reached. At this stage, on average 122 trials were rejected per subject (*SD* = 83.73). The remaining trials were submitted to a rank-reduced independent component analysis. That is, by decomposing a principal component subspace of the data, the number of components to be decomposed is reduced to match the number of rejected channels +1. This accounts for the rank deficiency in the data caused by the interpolation of rejected channels and the average reference procedure. To differentiate independent components reflecting brain sources from those reflecting non-brain sources, the automated classifier tool ICLabel [76] was applied. For each IC, ICLabel assigns a probability value to each of following classes: "brain", "eye", "muscle", "line noise", "channel noise", and "other". Components with a probability estimate of > 30% in the category 'eye' or < 30% in the category 'brain' are flagged for rejection. However, prior to removal, the obtained ICA decomposition is copied to the unaltered copy of the dataset obtained prior to ICA-based artefact identification (i.e., the reference dataset with a sampling rate of 1000 Hz and high-pass filtered at .01 Hz). The latter dataset is segmented into epochs, as described above. Then, the independent components previously flagged as "artifactual" are removed and their activities subtracted from the data. On average, 31.36 ICs were removed per subject (*SD* = 6.02). In a final step, trials that

still contained large fluctuations (±150 μV) are removed from the data, using the built-in EEGLAB function *pop_eegthresh()*. At this stage, on average 9 trials were rejected per subject (*SD* = 12.00).

4.7 Time-Frequency Decomposition

The time-frequency decomposition was obtain using the EEGLAB built-in STUDY functions, applying Morlet Wavelet Convolution. Specifically, the preprocessed single-trial EEG data was convolved with a series of complex Morlet wavelets, varying in frequency from 4 to 30 Hz in 52 logarithmically spaced steps. A complex Morlet wavelet can be described as a Gaussian-modulated complex sine wave, where the number of cycles determines the width of the tapering Gaussian. To account for the trade-off between temporal and frequency precision, the number of cycles increased linearly as a function of frequency by a factor of 0.5, starting from 3 cycles at the lowest frequency (4 Hz) and up to 11.25 cycles at the highest frequency (30 Hz). The resulting event-related spectral perturbations (ERSPs) ranged from -1082 to 1082 ms relative to sound onset. We did not subtract a spectral baseline.

4.8 Analysis

Behavioral data analysis was conducted using JASP (v.0.18.1.0[77]). EEG data analysis was conducted using custom-written MATLAB (R2023b and R2021b) scripts relying on the open-source toolboxes EEGLAB (v2021.1). Unless otherwise specified, all analyses were conducted separately for central and lateral sounds. For repeated-measures ANOVA (rmANOVA), we used Mauchly's test to assess the assumption of sphericity. In case of a violation ($p < .05$), Greenhouse-Geisser correction was applied. If appropriate, post-hoc paired sample-tests were corrected for multiple comparisons using either false discovery rate correction [78]. Corrected *p*-values are denoted as p_{corr}. For directional a-priori hypotheses, planned contrasts were computed. Partial eta squared (η_p^2) and Cohen's *d* are reported as effect sizes for rmANOVA and paired-sample *t*-tests, respectively. Cohen's *d* was computed, using the standard deviation of the difference score as a denominator. In MATLAB, Cohen's *d* was calculated using the toolbox 'Measures of Effect Sizes' [79].

For easier readability, statistical results of the omnibus tests and significant results of the post-hoc or planned contrasts are reported. All non-significant results can be taken from the JASP file available in our online OSF repository.

To check to see if the behavioral results were influenced by the strong bias of a part of the sample, we repeated the complete analysis without the biased participants. Participants were considered to have a strong response bias, when more than 90% or less than 10% of mid sounds were indicated as coming from the right side. Based on this criterion, we excluded five subjects, 3 of which had a strong left-ward bias and 2 had a strong right-ward bias. Detailed results can be taken from the respective JASP file available in our online OSF repository.

4.8.1 Behavioral Analysis

Central Sounds

For central sounds, participants were required to make a forced choice between a left versus right sound location. Accordingly, there are no correct responses. Instead, the proportion of

right-ward judgements served as a dependent variable to assess the influence of chemosensory stimulations on the response choice. Specifically, a 2-way rmANOVA with the within-subject factors *stimulation* (left nostril, right nostril, birhinal, auditory-only) and *sequence half* (first, second) was conducted.

In addition, reaction times to central sound localizations were analyzed using a 2-way rmANOVA with factors *sequence half* (first, second) and *stimulation* (congruent, incongruent, birhinal, auditory-only). Odorant stimulation could be either congruent with the given response (i.e., left nostril stimulation and left-ward response; right-nostril stimulation and right-ward response) or incongruent (i.e., left-nostril stimulation and right-ward responses; right-nostril stimulation and left-ward response). For the two control conditions (birhinal, auditory-only), response times were averaged across left and right button presses.

In addition, for both sets of analyses, planned one-sided contrasts were conducted to test our directional hypotheses based on results by Liang et al. (2022). Specifically, conditions with monorhinal stimulation were contrasted with the two control conditions. As JASP does not offer one-sided contrasts, the *p*-value was divided by 2 in case of a significant result in the direction of our hypothesis.

Lateral Sounds

The influence of chemosensory stimulation on the correct localization of lateral sounds were analyzed using a 3-way rmANOVA with the within-subject factors *stimulation* (congruent, incongruent, birhinal, auditory-only), *sound positions* (mid-out, far-out) and *sequence halves* (first, second). Note that, congruent and incongruent stimulation conditions refer to the side of the chemosensory stimulation relative to the actual sound location. That is, congruent trials include left-nostril stimulation and left responses as well as right-nostril stimulation and right responses, whereas incongruent trials include left-nostril stimulation and right responses as well as right-nostril stimulation and left-response. Mid-out sound positions refer to lateral sounds presented at +/-5° azimuth, while far-out sound positions include lateral sounds presented at +/-15° azimuth.

The influence of chemosensory stimulations on reaction times (RTs) to lateral sounds were analogously analyzed to the accuracy analysis by means of a 3-way rmANOVA with factor *stimulation* (congruent, incongruent, birhinal, auditory-only), *sound position* (mid-out, far- out) and *sequence halves* (first, second). Only correct responses were considered in this analysis of response times.

Again, for both analyses, planned one-sided contrasts were conducted guided by our hypotheses based on results by Liang et al. (2022).

4.8.2 Univariate analysis of alpha power lateralization

To obtain a time-resolved measure of posterior alpha power lateralization, EEG data from four left-hemispheric (i.e., PO7, P7, P3, PO3) and four right-hemispheric (i.e., PO8, P8, P4, PO4) channels were considered (Figure 2-A). Alpha power (8-12 Hz) was averaged across electrode sites on the same side as the focus of spatial attention (i.e., ipsilateral) and on the opposite side

(i.e. contralateral). To quantify the time-resolved lateralization of alpha power, the alpha lateralization index (ALI) was calculated as followed:

$$\frac{Contralateral\ power - \ ipsilateral\ power}{Contralateral\ power + \ ipsilateral\ power}$$

The analysis time-window to derive mean ALI values as input for a rmANOVA was determined based on a collapsed localizer approach [80]. First, the peak in the grand average waveform, collapsed across all conditions and subjects, was determined. Then, a 300 ms time window was centered on the respective peak value (i.e., peak +/- 150 ms). Subsequentially, mean ALI values were obtained per condition and subject.

Central Sounds

For the analysis of central sound-trials, the contralateral and ipsilateral electrode sites are assigned relative to the chosen response side (left vs. right). Accordingly, we assume that the focus of spatial attention shifts to the chosen response hemifield. To account for partially extremely unbalanced trial numbers across response categories, a weighted averaged was computed when collapsing across trials from different response categories.

First, to verify the presence of a significant lateralization of alpha power in response to a centrally presented sound that is classified as either right- or left-lateralized, irrespective of the odor-conditions, the grand-average data was tested against zero. To this end, a non-parametric cluster-corrected sign-permutation test was conducted, using the *cluster_test()* and *cluster_test_helper()* functions provided by[81]. The *cluster_test_helper()* function generates a null distribution by randomly flipping the sign of the input data of each participant with a probability of 50%. This procedure is repeated 10,000 times. The resulting distribution is submitted to the *cluster_test()* function, which identifies those clusters in the actual data that are greater than would we expected under the null hypothesis. The cluster-forming threshold as well as the cluster significance threshold were set to $p < .05$. Only post-stimulus time-points were considered as input data, since the pre-stimulus period in the full epochs (i.e., -1082 to 1082 ms relative to sound onset) strongly overlaps with the previous trial. Given that the alpha lateralization index is expected to be negative in case of a shift of attention towards the chosen response hemifield, the cluster-corrected sign-permutation test was one-sided.

Second, to test for differences in lateralization magnitude between conditions, mean ALI values were derived and submitted to a 1-way rmANOVA including the within-subject factor *stimulation* (congruent, incongruent, birhinal, sound-only). The collapsed localizer approach, described above, yielded an analysis time window in-between 389 ms to 689 ms relative to sound onset. Analogous to the behavioral data analysis, congruent chemosensory-sound stimulation refers to trials in which the chosen response (left vs. right) is in accordance with the stimulated nostril side. Accordingly, incongruent chemosensory-sound stimulation includes all trials in which the chosen response is incompatible with the stimulated nostril side (e.g., left-nostril stimulation and a right-ward response).

Lateral Sounds

For the analysis of lateral sounds, only correct responses are included in the analysis. Contralateral and ipsilateral electrode sites are assigned according to the physical sound position. The collapsed localizer approach, described above, yielded an analysis time window ranging from 309 to 609 ms post-sound onset. Mean ALI values were submitted to a rmANOVA including the factors *stimulation* (right-nostril, left-nostril, birhinal, sound-only) and *sound position* (far-out, mid-out). To follow-up on significant interaction effects, two-sided paired sample *t*-tests were conducted and corrected for multiple comparisons. Due to a limited number of trials (i.e., ~30 trials per cell), the factor *sequence half* (first, second) was omitted from the primary EEG analysis. However, for comparability with the behavioral analysis, a supplementary 3-way rmANOVA was run to check for potential interactions with *sequence half* (see supplementary material, S1).

4.8.3 Multivariate pattern analysis of alpha-band topographies

Adopting the classifier routine as described in Klatt and colleagues (2022; modified based on scripts from Bae & Luck, 2018), we decoded the spatial location the stimuli in the sound sequence (left vs. right) based on the scalp distribution of alpha-band EEG power (Figure 3-A). The decoding procedure was applied separately to the four stimulation conditions (auditory-only, odor-congruent, odor-incongruent, birhinal). To optimize the available number of trials, we opted for a binary classification of left versus right sound locations instead of decoding the exact sound location (far-left, mid-left, far-right, mid-right). Trials in which the sound was presented in a central, non-lateralized position were excluded from this analysis. Alpha-band ERSPs (8-12 Hz) served as input data, including all time points between -200 and 1000 ms relative to sound onset. This results in a 4-dimensional data matrix for each participant, including the dimensions of time (167 time points), location (2 different categories), trial (varies depending on the subject; auditory-only: 62-128 trials per location, birhinal: 26-64 trials per location, congruent: 30 – 64 trials per location, incongruent: 25 – 64 trials per location), and electrode site (65 scalp channels). Decoding was performed separately for each of the 167 time points, using a combination of a support vector machine (SVM) and error-correcting output codes (ECOC; Dietterich & Balkiri, 1995) with a one versus one coding scheme, as implemented in the *fitcecoc()* MATLAB function. Classifications were performed within subjects and using trial averages rather than single-trial data. The latter has been shown to result in higher (although more variable) decoding accuracies [83], due to increased signal-to-noise ratio in the classifier input. Specifically, at each time point, 50 iterations of the classification analysis were performed; on each iteration, the data were sorted into two 'location bins', containing only trials in which the sound was presented in the right or left hemifield, respectively. In each location bin, the trials were randomly divided into three equally sized sets of trials. To ensure that an equal number of trials was assigned to each of the three sets, the minimum number of trials per subject for a given location bin was determined (denoted as *n*), and *n* / 3 trials were assigned to each set. In case the total trial number for a given location was not evenly divisible by three, excess trials were randomly omitted. The trials for a given location bin were averaged, resulting in a matrix of 3 (subsample averages) x 2 (location bins) x 64 (electrodes) to be

analyzed for each time point. Two of the three subsample averages (for each target location) served as the training set, while the remaining subsample average (for each target location) was assigned to the testing dataset. In the training phase, the data from the two (of the total three) subsample averages were simultaneously submitted to the ECOC model with known location labels to train a binary SVM model, which learns to discriminate between trials with a right-sided versus left-sided sounds. Subsequently, in the test phase the unused data (i.e., the subsample averages that were reserved for testing) was passed to the trained SVM, using the MATLAB predict() function, to classify whether the sound was presented on the left or right side in each of the subsample averages. Essentially, the output of the *predict()* function provides a location label for each of the two remaining subsample averages in the testing dataset. By comparing the true location labels to the predicted location labels, decoding accuracy was computed. Decoding was considered correct if the classifier correctly indicated the side of sound presentation. Thus, chance level decoding accuracy was at 50%. This training-and-testing process was applied three times such that each subsample average served as the testing dataset once. Finally, decoding accuracy was collapsed across the two locations, the three cycles of cross-validation, and the 50 iterations, resulting in a decoding percentage for each time point. After obtaining a decoding percentage for all time points of interest, a five-point moving average was applied to smooth the averaged decoding accuracy values and to minimize noise.

Statistical analysis of decoding accuracy

To assess the statistical significance of within-condition decoding accuracy, we applied a non-parametric cluster-based permutation analysis, adopting the analysis code provided by Bae Luck, 2019). At each time point, the average decoding accuracy across subjects was compared to chance level (i.e., 50%) by conducting a one-sided one sample *t*-tests. This is justified because SVM decoding does not produce meaningful below-chance decoding results. Then, clusters of at least two adjacent time points with a significant single-point *t*-test (i.e. $p < .05$) were identified. The *t*-values within a given cluster were summed, constituting the so-called cluster mass. To determine whether a particular cluster mass value is greater than what can be expected by chance, we constructed a null distribution of cluster-level *t*-mass values. Critically, to reduce computation time, we randomly permuted the target labels at the stage of testing the decoding output, rather than prior to training the classifier. Specifically, from an array containing all possible target labels (1 vs. 2), we randomly sampled an integer as the simulated response of the classifier for a given sound location. If the classifier response matched the true sound location, it was considered correct. This yields an estimate of the decoding accuracy that would by obtained by chance if the decoder randomly guessed the sound location. Critically, to reflect the temporal autocorrelation of the continuous EEG data, the same randomly sampled target position label was used for all time points in a given subaverage. Overall, this sampling procedure was repeated 300 times (2 locations x 3 cross-validations x 50 iterations) and for each time point of interest in-between -200 ms to 1000 ms. The scores for each time point were averaged to obtain the mean simulated decoding accuracy, resulting in a time series of decoding accuracy values. Analogous to the procedure that was applied to the actual EEG

data, the latter was smoothed using a five-point running average filter. The procedure was repeated 25 times, to obtain a simulated decoding accuracy time series for each of our 25 participants. Then, using the simulated decoding accuracy time series, the maximum cluster mass was computed, using the procedure described above. That is, if there was more than one cluster of significant *t*-values, the mass of the largest cluster was selected.

Finally, this procedure (i.e., simulating decoding accuracy that would be obtained by chance) was iterated 10,000 times to produce a null distribution of cluster mass values. For each cluster in the decoding results, the obtained cluster *t* mass was compared to the distribution of cluster *t* mass values that was constructed under the assumption that the null hypothesis is true. If the observed cluster *t* mass value was larger than the 95th quantile of the null distribution (i.e., α = .05, one-tailed), the null hypothesis was rejected, and decoding accuracy was considered above chance. Note that this procedure was separately applied to all stimulation conditions (auditory-only, congruent, incongruent, birhinal).

To find the *p*-value associated with a specific cluster, we examined where within the null distribution does each observed cluster *t* mass value fall. That is, the *p*-value was based on the inverse percentile (computed using the *invprctile()* function) of the observed cluster-level *t*-mass within the null distribution. If the observed cluster-level *t*-mass value exceeded the maximum cluster-level *t*-mass of the simulated null distribution, the respective *p*-value is reported as $p < 10^{-4}$. The latter corresponds to the resolution of the null distribution (i.e., 1 / number of permutations).

Statistical differences in decoding accuracy between stimulation conditions

To investigate whether or not the decoding of sound location is influenced by concurrent odorant stimulation, decoding accuracy in the four stimulation conditions was compared, using a two-sided cluster-corrected sign-permutation test (cf. section 4.8.2). As input data, the same time window that was also used for the statistical analysis of decoding accuracy within conditions was selected (i.e., -200 ms to 1000 ms). This yields a total of 6 pair-wise comparisons. In addition, to assess the overall difference in decoding ability within the post-stimulus period, average decoding accuracy in-between 338 and 638 ms was submitted to a two-sided permutation test. To this end, the *GroupPermTest()* function, provided by [81], was applied (using nSims = 10,000 permutations). The analysis time window corresponds to a +/- 150 ms window surrounding the decoding accuracy peak in the grand average waveform across all four conditions.

4.9 Data and code availability

All data and code used to generate the present findings will be made publicly available on the Open Science Framework (OSF) upon acceptance for publication of this manuscript.

5. Authors Contribution

Conceptualization, C.H. and L.K.; Methodology, C.H. and L.K.; Formal Analysis, C.H. and L.K.; Investigation, C.H. and L.K.; Data Curation: C.H. and L.K.; Writing – Original Draft, C.H. and L.K., Writing – Review & Editing, C.H. and L.K.; Visualization, C.H. and L.K.

6. Declaration of interests

The authors declare no competing interests.

7. Acknowledgements

We would like to thank J. Reiser, A. Hijazi, as well as S. Kattan for their help with EEG data collection. In addition, we would like to thank M. Porta and J. Reinders for the preparation of isopropanol samples as well as N. Koschmieder for assistance with spirometry data acquisition. Finally, we are grateful for S. Getzmann's and C. van Thriel's contributions in discussions concerning the design of the paradigm.

8. References

1. Chen, L., and Vroomen, J. (2013). Intersensory binding across space and time: A tutorial review. Atten. Percept. Psychophys. *75*, 790–811. 10.3758/s13414-013-0475-4.
2. Bruns, P., and Röder, B. (2010). Tactile capture of auditory localization: an event-related potential study. Eur. J. Neurosci. *31*, 1844–1857. 10.1111/j.1460-9568.2010.07232.x.
3. Kuang, S., and Zhang, T. (2014). Smelling directions: Olfaction modulates ambiguous visual motion perception. Sci. Rep. *4*, 5796. 10.1038/srep05796.
4. Wu, Y., Chen, K., Ye, Y., Zhang, T., and Zhou, W. (2020). Humans navigate with stereo olfaction. Proc. Natl. Acad. Sci. U. S. A., 1–7. 10.1073/pnas.2004642117.
5. Liang, K., Wang, W., Lei, X., Zeng, H., Gong, W., Lou, C., and Chen, L. (2022). Odor-induced sound localization bias under unilateral intranasal trigeminal stimulation. Chem. Senses *47*, bjac029. 10.1093/chemse/bjac029.
6. Croy, I., Schulz, M., Blumrich, A., Hummel, C., Gerber, J., and Hummel, T. (2014). Human olfactory lateralization requires trigeminal activation. NeuroImage *98*, 289–295. 10.1016/j.neuroimage.2014.05.004.
7. Kleemann, A.M., Albrecht, J., Schöpf, V., Haegler, K., Kopietz, R., Hempel, J.M., Linn, J., Flanagin, V.L., Fesl, G., and Wiesmann, M. (2009). Trigeminal perception is necessary to localize odors. Physiol. Behav. *97*, 401–405. 10.1016/j.physbeh.2009.03.013.
8. Kobal, G., Van Toller, S., and Hummel, T. (1989). Is there directional smelling? Experientia *45*, 130–132.
9. Rihs, T.A., Michel, C.M., and Thut, G. (2007). Mechanisms of selective inhibition in visual spatial attention are indexed by α-band EEG synchronization. Eur. J. Neurosci. *25*, 603–610. 10.1111/j.1460-9568.2007.05278.x.
10. Sauseng, P., Klimesch, W., Stadler, W., Schabus, M., Doppelmayr, M., Hanslmayr, S., Gruber, W.R., and Birbaumer, N. (2005). A shift of visual spatial attention is selectively associated with human EEG alpha activity. Eur. J. Neurosci. *22*, 2917–2926. 10.1111/j.1460-9568.2005.04482.x.
11. Thut, G., Nietzel, A., Brandt, S.A., and Pascual-Leone, A. (2006). α-Band Electroencephalographic Activity over Occipital Cortex Indexes Visuospatial Attention Bias and Predicts Visual Target Detection. J. Neurosci. *26*, 9494–9502. 10.1523/JNEUROSCI.0875-06.2006.
12. Yamagishi, N., Goda, N., Callan, D.E., Anderson, S.J., and Kawato, M. (2005). Attentional shifts towards an expected visual target alter the level of alpha-band oscillatory activity in the human calcarine cortex. Cogn. Brain Res. *25*, 799–809. 10.1016/j.cogbrainres.2005.09.006.
13. Klatt, L.-I., Getzmann, S., Begau, A., and Schneider, D. (2020). A dual mechanism

underlying retroactive shifts of auditory spatial attention: dissociating target- and distractor-related modulations of alpha lateralization. Sci. Rep. *10*, 13860. 10.1038/s41598-020-70004-2.

14. Myers, N.E., Walther, L., Wallis, G., Stokes, M.G., and Nobre, A.C. (2015). Temporal Dynamics of Attention during Encoding versus Maintenance of Working Memory: Complementary Views from Event-related Potentials and Alpha-band Oscillations. J. Cogn. Neurosci. *27*, 492–508. 10.1162/jocn_a_00727.
15. Poch, C., Capilla, A., Hinojosa, J.A., and Campo, P. (2017). Selection within working memory based on a color retro-cue modulates alpha oscillations. Neuropsychologia *106*, 133–137. 10.1016/j.neuropsychologia.2017.09.027.
16. Schneider, D., Mertes, C., and Wascher, E. (2016). The time course of visuo-spatial working memory updating revealed by a retro-cuing paradigm. Sci. Rep. *6*, 21442. 10.1038/srep21442.
17. Bacigalupo, F., and Luck, S.J. (2019). Lateralized Suppression of Alpha-Band EEG Activity As a Mechanism of Target Processing. J. Neurosci. *39*, 900–917. 10.1523/JNEUROSCI.0183-18.2018.
18. Getzmann, S., Klatt, L.-I., Schneider, D., Begau, A., and Wascher, E. (2020). EEG correlates of spatial shifts of attention in a dynamic multi-talker speech perception scenario in younger and older adults. Hear. Res. *398*, 108077. 10.1016/j.heares.2020.108077.
19. Klatt, L.-I., Getzmann, S., Wascher, E., and Schneider, D. (2018). Searching for auditory targets in external space and in working memory: Electrophysiological mechanisms underlying perceptual and retroactive spatial attention. Behav. Brain Res. *353*, 98–107. 10.1016/j.bbr.2018.06.022.
20. Popov, T., Gips, B., Weisz, N., and Jensen, O. (2023). Brain areas associated with visual spatial attention display topographic organization during auditory spatial attention. Cereb. Cortex *33*, 3478–3489. 10.1093/cercor/bhac285.
21. Tune, S., Wöstmann, M., and Obleser, J. (2018). Probing the limits of alpha power lateralisation as a neural marker of selective attention in middle-aged and older listeners. Eur. J. Neurosci. *48*, 2537–2550. 10.1111/ejn.13862.
22. Wöstmann, M., Alavash, M., and Obleser, J. (2019). Alpha Oscillations in the Human Brain Implement Distractor Suppression Independent of Target Selection. J. Neurosci. *39*, 9797–9805. 10.1523/JNEUROSCI.1954-19.2019.
23. Deng, Y., Choi, I., and Shinn-Cunningham, B. (2020). Topographic specificity of alpha power during auditory spatial attention. NeuroImage *207*, 116360. 10.1016/j.neuroimage.2019.116360.
24. Banerjee, S., Snyder, A.C., Molholm, S., and Foxe, J.J. (2011). Oscillatory Alpha-Band Mechanisms and the Deployment of Spatial Attention to Anticipated Auditory and Visual Target Locations: Supramodal or Sensory-Specific Con18:00trol Mechanisms? J. Neurosci. *31*, 9923–9932. 10.1523/JNEUROSCI.4660-10.2011.
25. Chambers, C.D., Stokes, M.G., and Mattingley, J.B. (2004). Modality-Specific Control of Strategic Spatial Attention in Parietal Cortex. Neuron *44*, 925–930. 10.1016/j.neuron.2004.12.009.
26. Bae, G.-Y., and Luck, S.J. (2018). Dissociable Decoding of Spatial Attention and Working Memory from EEG Oscillations and Sustained Potentials. J. Neurosci. *38*, 409–422. 10.1523/JNEUROSCI.2860-17.2017.
27. Foster, J.J., Sutterer, D.W., Serences, J.T., Vogel, E.K., and Awh, E. (2016). The topography of alpha-band activity tracks the content of spatial working memory. J. Neurophysiol. *115*, 168–177. 10.1152/jn.00860.2015.

28. Foster, J.J., Sutterer, D.W., Serences, J.T., Vogel, E.K., and Awh, E. (2017). Alpha-Band Oscillations Enable Spatially and Temporally Resolved Tracking of Covert Spatial Attention. Psychol. Sci. *28*, 929–941. 10.1177/0956797617699167.
29. Klatt, L.-I., Getzmann, S., and Schneider, D. (2022). Attentional modulations of alpha power are sensitive to the task-relevance of auditory spatial information. Cortex *153*, 1–20. https://doi.org/10.1016/j.cortex.2022.03.022.
30. Sutterer, D.W., Foster, J.J., Adam, K.C.S., Vogel, E.K., and Awh, E. (2019). Item-specific delay activity demonstrates concurrent storage of multiple active neural representations in working memory. PLOS Biol. *17*, e3000239. 10.1371/journal.pbio.3000239.
31. Foxe, J.J., Simpson, G.V., and Ahlfors, S.P. (1998). Parieto-occipital ~1 0Hz activity reflects anticipatory state of visual attention mechanisms: NeuroReport *9*, 3929–3933. 10.1097/00001756-199812010-00030.
32. Mazaheri, A., Van Schouwenburg, M.R., Dimitrijevic, A., Denys, D., Cools, R., and Jensen, O. (2014). Region-specific modulations in oscillatory alpha activity serve to facilitate processing in the visual and auditory modalities. NeuroImage *87*, 356–362. 10.1016/j.neuroimage.2013.10.052.
33. van Diepen, R.M., and Mazaheri, A. (2017). Cross-sensory modulation of alpha oscillatory activity: suppression, idling, and default resource allocation. Eur. J. Neurosci. *45*, 1431–1438. 10.1111/ejn.13570.
34. van Ede, F., Jensen, O., and Maris, E. (2017). Supramodal Theta, Gamma, and Sustained Fields Predict Modality-specific Modulations of Alpha and Beta Oscillations during Visual and Tactile Working Memory. J. Cogn. Neurosci. *29*, 1455–1472. 10.1162/jocn_a_01129.
35. Hummel, T. (2000). Assessment of intranasal trigeminal function. Int. J. Psychophysiol. *36*, 147–155. 10.4193/Rhin15.002.
36. Hummel, T., and Frasnelli, J. (2019). Chapter 8 - The intranasal trigeminal system. In Handbook of Clinical Neurology, R. L. Doty, ed. (Elsevier), pp. 119–134. https://doi.org/10.1016/B978-0-444-63855-7.00008-3.
37. Klatt, L.-I., Getzmann, S., Wascher, E., and Schneider, D. (2018). The contribution of selective spatial attention to sound detection and sound localization: Evidence from event-related potentials and lateralized alpha oscillations. Biol. Psychol. *138*, 133–145. 10.1016/j.biopsycho.2018.08.019.
38. Wöstmann, M., Vosskuhl, J., Obleser, J., and Herrmann, C.S. (2018). Opposite effects of lateralised transcranial alpha versus gamma stimulation on auditory spatial attention. Brain Stimulat. *11*, 752–758. 10.1016/j.brs.2018.04.006.
39. Pause, B.M., Sojka, B., and Ferstl, R. (1997). Central processing of odor concentration is a temporal phenomenon as revealed by chemosensory event-related potentials (CSERP). Chem. Senses *22*, 9–26. 10.1093/chemse/22.1.9.
40. Luck, S.J. (2014). An introduction to the event-related potential technique 2nd ed. (MIT Press).
41. Carlson, K.S., Xia, C.Z., and Wesson, D.W. (2013). Encoding and Representation of Intranasal CO2 in the Mouse Olfactory Cortex. J. Neurosci. *33*, 13873–13881. 10.1523/JNEUROSCI.0422-13.2013.
42. Hummel, T., Livermore, A., Hummel, C., and Kobal, G. (1992). Chemosensory event-related potentials in man: relation to olfactory and painful sensations elicited by nicotine. Electroencephalogr. Clin. Neurophysiol. Potentials Sect. *84*, 192–195. 10.1016/0168-5597(92)90025-7.
43. Zhou, W., and Chen, D. (2009). Fear-Related Chemosignals Modulate Recognition of Fear in Ambiguous Facial Expressions. Psychol. Sci. *20*, 177–183. 10.1111/j.1467-

9280.2009.02263.x.

44. Zhou, W., Jiang, Y., He, S., and Chen, D. (2010). Olfaction Modulates Visual Perception in Binocular Rivalry. Curr. Biol. *20*, 1356–1358. 10.1016/j.cub.2010.05.059.
45. Blake, R., and O'Shea, R.P. (2017). Binocular Rivalry. In Reference Module in Neuroscience and Biobehavioral Psychology (Elsevier), p. B9780128093245221846. 10.1016/B978-0-12-809324-5.22184-6.
46. Macaluso, E., and Driver, J. (2001). Spatial attention and crossmodal interactions between vision and touch. Neuropsychologia *39*, 1304–1316. 10.1016/S0028-3932(01)00119-1.
47. Spence, C., Kettenmann, B., Kobal, G., and McGlone, F.P. (2001). Shared Attentional Resources for processing Visual and Chemosensory Information. Q. J. Exp. Psychol. Sect. A *54*, 775–783. 10.1080/713755985.
48. Frasnelli, J., Lundström, J.N., Schöpf, V., Negoias, S., Hummel, T., and Lepore, F. (2012). Dual processing streams in chemosensory perception. Front. Hum. Neurosci. *6*, 1–9. 10.3389/fnhum.2012.00288.
49. Calvert, G.A., Hansen, P.C., Iversen, S.D., and Brammer, M.J. (2001). Detection of Audio-Visual Integration Sites in Humans by Application of Electrophysiological Criteria to the BOLD Effect. NeuroImage *14*, 427–438. 10.1006/nimg.2001.0812.
50. Boyle, J.A., Frasnelli, J., Gerber, J., Heinke, M., and Hummel, T. (2007). Cross-modal integration of intranasal stimuli: A functional magnetic resonance imaging study. Neuroscience *149*, 223–231. 10.1016/j.neuroscience.2007.06.045.
51. Maeder, P.P., Meuli, R.A., Adriani, M., Bellmann, A., Fornari, E., Thiran, J.-P., Pittet, A., and Clarke, S. (2001). Distinct Pathways Involved in Sound Recognition and Localization: A Human fMRI Study. NeuroImage *14*, 802–816. 10.1006/nimg.2001.0888.
52. Rauschecker, J.P., and Tian, B. (2000). Mechanisms and streams for processing of "what" and "where" in auditory cortex. Proc. Natl. Acad. Sci. *97*, 11800–11806. 10.1073/pnas.97.22.11800.
53. Green, A.M., and Angelaki, D.E. (2010). Multisensory integration: resolving sensory ambiguities to build novel representations. Curr. Opin. Neurobiol. *20*, 353–360. 10.1016/j.conb.2010.04.009.
54. Wöstmann, M., Maess, B., and Obleser, J. (2020). Orienting auditory attention in time: Lateralized alpha power reflects spatio-temporal filtering. NeuroImage, 117711. 10.1016/j.neuroimage.2020.117711.
55. Kerlin, J.R., Shahin, A.J., and Miller, L.M. (2010). Attention gain control of ongoing cortical speech representations in a "cocktail party." J. Neurosci. *30*, 620–628. 10.1523/JNEUROSCI.3631-09.2010.
56. Ischer, M., Coppin, G., De Marles, A., Essellier, M., Porcherot, C., Cayeux, I., Margot, C., Sander, D., and Delplanque, S. (2021). Exogenous capture of visual spatial attention by olfactory-trigeminal stimuli. PLOS ONE *16*, e0252943. 10.1371/journal.pone.0252943.
57. La Buissonnière-Ariza, V., Frasnelli, J., Collignon, O., and Lepore, F. (2012). Olfactory priming leads to faster sound localization. Neurosci. Lett. *506*, 188–192. 10.1016/j.neulet.2011.11.002.
58. Wudarczyk, O.A., Habel, U., Turetsky, B.I., Gur, R.E., Kellermann, T., Schneider, F., and Moessnang, C. (2016). Follow your nose: Implicit spatial processing within the chemosensory systems. J. Exp. Psychol. Hum. Percept. Perform. *42*, 1780–1792. 10.1037/xhp0000261.
59. Klatt, L.-I., Getzmann, S., and Schneider, D. (2022). Attentional modulations of alpha power are sensitive to the task-relevance of auditory spatial information. Cortex *153*, 1–20. 10.1016/j.cortex.2022.03.022.

60. Hucke, C.I., Heinen, R.M., Wascher, E., and van Thriel, C. (2023). Trigeminal stimulation is required for neural representations of bimodal odor localization: A time-resolved multivariate EEG and fNIRS study. NeuroImage *269*, 119903. https://doi.org/10.1016/j.neuroimage.2023.119903.
61. Bonath, B., Noesselt, T., Martinez, A., Mishra, J., Schwiecker, K., Heinze, H.-J., and Hillyard, S.A. (2007). Neural Basis of the Ventriloquist Illusion. Curr. Biol. *17*, 1697–1703. 10.1016/j.cub.2007.08.050.
62. Mills, A.W. (1960). Lateralization of High-Frequency Tones. J. Acoust. Soc. Am. *32*, 132–134. 10.2475/ajs.s3-11.66.442.
63. Moessnang, C., Finkelmeyer, A., Vossen, A., Schneider, F., and Habel, U. (2011). Assessing Implicit Odor Localization in Humans Using a Cross-Modal Spatial Cueing Paradigm. PLOS ONE *6*, e29614. 10.1371/journal.pone.0029614.
64. Campbell, J.I.D., and Thompson, V.A. (2012). MorePower 6.0 for ANOVA with relational confidence intervals and Bayesian analysis. Behav. Res. Methods *44*, 1255–1265. 10.3758/s13428-012-0186-0.
65. Graham, B.L., Steenbruggen, I., Miller, M.R., Barjaktarevic, I.Z., Cooper, B.G., Hall, G.L., Hallstrand, T.S., Kaminsky, D.A., McCarthy, K., McCormack, M.C., et al. (2019). Standardization of Spirometry 2019 Update. An Official American Thoracic Society and European Respiratory Society Technical Statement. Am. J. Respir. Crit. Care Med. *200*, e70–e88. 10.1164/rccm.201908-1590ST.
66. Hummel, T., Kobal, G., Gudziol, H., and Mackay-Sim, A. (2007). Normative data for the "Sniffin' Sticks" including tests of odor identification, odor discrimination, and olfactory thresholds: an upgrade based on a group of more than 3,000 subjects. Rhinology *264*, 237–243. 10.1007/s00405-006-0173-0.
67. Oleszkiewicz, A., Schriever, V.A., Croy, I., Hähner, A., and Hummel, T. (2019). Updated Sniffin' Sticks normative data based on an extended sample of 9139 subjects. Eur. Arch. Otorhinolaryngol. *276*, 719–728. 10.1007/s00405-018-5248-1.
68. Olusanya, B.O., Davis, A.C., and Hoffman, H.J. (2019). Hearing loss grades and the International classification of functioning, disability and health. Bull. World Health Organ. *97*, 725–728. 10.2471/BLT.19.230367.
69. Smeets, M., Mauté, C., and Dalton, P. (2002). Acute Sensory Irritation from Exposure to Isopropanol (2-Propanol) at TLV in Workers and Controls: Objective versus Subjective Effects. Ann. Occup. Hyg. *46*, 359–373. 10.1093/annhyg/mef054.
70. Smeets, M., and Dalton, P. (2002). Perceived odor and irritation of isopropanol: a comparison between naïve controls and occupationally exposed workers. Int. Arch. Occup. Environ. Health *75*, 541–548. 10.1007/s00420-002-0364-y.
71. Hucke, C.I., Pacharra, M., Reinders, J., and van Thriel, C. (2018). Somatosensory response to trigeminal stimulation: A functional near-infrared spectroscopy (fNIRS) study. Sci. Rep. *8*, 13771. 10.1038/s41598-018-32147-1.
72. Hucke, C.I., Heinen, R.M., Pacharra, M., Wascher, E., and van Thriel, C. (2021). Spatiotemporal Processing of Bimodal Odor Lateralization in the Brain Using Electroencephalography Microstates and Source Localization. Front. Neurosci. *14*, 620723. 10.3389/fnins.2020.620723.
73. Kobal, G. (1981). Elektrophysiologische Untersuchungen des menschlichen Geruchssinns (Thieme Verlag).
74. Delorme, A., and Makeig, S. (2004). EEGLAB: An open source toolbox for analysis of single-trial EEG dynamics including independent component analysis. J. Neurosci. Methods *134*, 9–21. 10.1016/j.jneumeth.2003.10.009.

75. Winkler, I., Debener, S., Muller, K.-R., and Tangermann, M. (2015). On the influence of high-pass filtering on ICA-based artifact reduction in EEG-ERP. In 2015 37th Annual International Conference of the IEEE Engineering in Medicine and Biology Society (EMBC) (IEEE), pp. 4101–4105. 10.1109/EMBC.2015.7319296.
76. Pion-Tonachini, L., Kreutz-Delgado, K., and Makeig, S. (2019). ICLabel: An automated electroencephalographic independent component classifier, dataset, and website. NeuroImage *198*, 181–197. 10.1016/j.neuroimage.2019.05.026.
77. JASP Team JASP. Version 0.18.1.
78. Benjamini, Y., and Hochberg, Y. (1995). Controlling the false discovery rate: A practical and powerful approach to multiple testing. J. R. Stat. Soc. *57*, 289–300. 10.2307/2346101.
79. Hentschke, H., and Stüttgen, M.C. (2011). Computation of measures of effect size for neuroscience data sets. Eur. J. Neurosci. *34*, 1887–1894. 10.1111/j.1460-9568.2011.07902.x.
80. Luck, S.J., and Gaspelin, N. (2017). How to Get Statistically Significant Effects in Any ERP Experiment (and Why You Shouldn't). Psychophysiology *54*, 146–157. 10.1111/psyp.12639.
81. Wolff, M.J., Jochim, J., Akyürek, E.G., and Stokes, M.G. (2017). Dynamic hidden states underlying working-memory-guided behavior. Nat. Neurosci. *20*, 864–871. 10.1038/nn.4546.
82. Dietterich, T.G., and Balkiri, G. (1995). Solving Multiclass Learning Problems via Error-Correcting Output Codes. J. Artifical Intell. Res. *2*, 263–286.
83. Adam, K.C.S., Vogel, E.K., and Awh, E. (2020). Multivariate analysis reveals a generalizable human electrophysiological signature of working memory load. Psychophysiology *57*, 1–17. 10.1111/psyp.13691.
84. Bae, G.-Y., and Luck, S.J. (2019). Appropriate Correction for Multiple Comparisons in Decoding of ERP Data: A Re-Analysis of Bae & Luck (2018) (Neuroscience) 10.1101/672741.

Supplementary Material

S1. Alpha Lateralization Index (ALI): 4 x 2 x 2 rmANOVA including the factors *condition*, *sound position*, and *sequence half.*

	DF	**F**	**p**	**n_p^2**
Condition	[3, 72]	1.0478	.377	0.042
Sound Position	[1, 24]	11.622	.002**	0.326
Sequence Half	[1, 24]	0.002	.963	< 0.001
Condition x Sound Position	**[3,72]**	**2.904**	**.041***	**0.108**
Condition x Sequence Half	[3,72]	0.121	.947	0.005
Sound Position x Sequence Half	[1,24]	5.218	.031*	0.179
Condition x Sound Position x Sequence Half	[3,72]	1.323	.274	0.052